

Search for Periodic Radio Signals from Double Neutron Star System Companions Using the Fast Folding Algorithm

Wenze Li¹, Zhichen Pan^{2,3,4,5}, Lei Qian^{2,3,4,5}, Liyun Zhang^{1,6}, Yujie Chen¹, Dejiang Yin¹,
Baoda Li¹, Yinfeng Dai^{7,8}, Yaowei Li⁹, Dongyue Jiang¹, Qiaoli Hao², Menglin Huang²,
Xingyi Wang², Xianghua Niu², Minglei Guo², Jinyou Song² and Shuangyuan Chen²

¹ College of Physics, Guizhou University, Guiyang 550025, China; *liy_zhang@hotmail.com*

² National Astronomical Observatories, Chinese Academy of Sciences, Beijing 100101, China;
panzc@nao.cas.cn; lqian@nao.cas.cn

³ Guizhou Radio Astronomical Observatory, Guizhou University, Guiyang 550025, China

⁴ College of Astronomy and Space Sciences, University of Chinese Academy of Sciences, Beijing
100049, China

⁵ Key Laboratory of Radio Astronomy, Chinese Academy of Sciences, Beijing 100101, China

⁶ International Centre of Supernovae, Yunnan Key Laboratory, Kunming 650216, China

⁷ School of Physics and Astronomy, Beijing Normal University, Beijing 100875, China

⁸ Department of Physics, Faculty of Arts and Sciences, Beijing Normal University, Zhuhai 519087, China

⁹ Department of Physics, School of Physics and Electronics, Hunan Normal University, Changsha
410081, China

Abstract As most of the companions in the double neutron star systems should be normal pulsars, the Fast Folding Algorithm (FFA), which is suitable for finding these long spin period pulsars, was used to search their possible radio signals. A time domain resampling code PYSOLATOR was used to maximize the available data length by removing the orbital modulation. We collected and processed 272.2 hours observational data taken by the Five-hundred-meter Aperture Spherical radio Telescope (FAST) for the 13 double neutron star systems in its sky. The signal-to-noise ratios of known pulsar signals are obviously improved by this search method, including the detection of a faint pulsar signal which only saw by folding the data. Unfortunately, no companion signals were found among all the 197962 candidates. Geodetic precession of the orbit could enhance detectability in future observations.

Key words: methods: data analysis - stars: neutron - pulsars: individual - binaries: close

1 INTRODUCTION

A double neutron star (DNS) system consists of two neutron stars, and normally at least one of which can be observed as a pulsar. The discovery of the first double neutron star system, B1913+16 (Hulse & Taylor

1975), indirectly confirmed the existence of gravitational waves (Taylor & Weisberg 1982) and provides an ideal laboratory for testing gravitational theories. Among hundreds of binary pulsar systems, 24 have been confirmed as DNS systems and with 11 more being candidates¹. If the periodic signals from both neutron stars can be observed, such a DNS was called a double pulsar.

The J0737-3039A/B binary system is the first and only double pulsar till now (Burgay et al. 2003; Lyne 2004). It is with a short orbital period $P_b = 2.4$ hours) and moderate eccentricity $e = 0.088$). The pulsars A and B have spin periods of 22.7 ms and 2.7 s, respectively. It is one of the best probes for validating general relativity and other theories of gravity in the strong regime field (Kramer & Stairs 2008). The five Keplerian parameters (Orbital Period P_b , Projected Semi-major Axis x , Eccentricity e , Longitude of Periastron ω_0 , Epoch of Periastron T_0) of each pulsar and seven post-Keplerian parameters (Periastron Advance $\dot{\omega}$, Einstein Delay γ , Shapiro Delay Range r , Shapiro Delay Shape s , Orbital Decay \dot{P}_b , Relativistic Orbital Deformation δ_θ , Spin Precession of B Ω_B^{spin}) in this system were detected (Kramer et al. 2021). The orbital decay rate \dot{P}_b agrees with the General Relativity's gravitational radiation prediction within 1.3×10^{-4} , a precision ~ 25 times that of the Hulse–Taylor pulsar (Kramer et al. 2021). In addition, double pulsar systems have unique significance for binary star evolution (Tauris & van den Heuvel 2006; Tauris et al. 2017), gravitational wave detection (Abbott et al. 2017), neutron star internal structure and equation of state (Lattimer & Prakash 2016), and extreme-environment plasma and magnetosphere (Breton et al. 2008).

Since the discovery of the DNS system, detecting more such systems has remained a long-standing ambition in pulsar surveys. The Five-hundred-meter Aperture Spherical radio Telescope (FAST, Nan et al. 2011) is the largest single-dish radio telescope, offering exceptional sensitivity for detecting such objects. It has discovered over 1000 pulsars, including 5 DNSs among approximately 150 new binary systems: J1953+1847D (Lian et al. 2025) in globular cluster M71, J1901+0658 (Su et al. 2024), J0528+3529, J1844-0128(Wang et al. 2025), and J2150+3427 (Wu et al. 2023) in Galactic field. It is estimated that more than 100 DNS systems should be discovered by the FAST and the Square Kilometre Array (SKA) (Keane et al. 2015). The second double pulsar system may be detectable with FAST using the FFA.

Most pulsars in known DNS systems are recycled, while their companions are considered to be normal, long-period pulsars according to pulsar evolution theory (e.g. Tauris et al. 2017). The Fast Folding Algorithm (FFA) is a phase-coherent search method that detects periodic signals by directly folding time series (Staelin 1969). Compared to the search pipeline based one Fast Fourier Transform (FFT), FFA is more sensitive to pulse signals with long periods and low duty cycles (Morello et al. 2020), and was successfully used to find new pulsars in FAST data (e.g., the slowest globular cluster pulsar M15L, $P \sim 3961$ ms, Wu et al. 2024). The FFA also has an exceptionally high detection rate (93.5%) and demonstrates superior sensitivity to weak signals even millisecond pulsars (Li et al. 2025). Therefore, FFA should be the suitable search algorithm to search for the companion periodic signals of DNS systems.

In this study, we employed the FFA to search for companion signals in DNS systems in the FAST sky. The structure of this paper is as follows: Section 2 describes the data and reduction process, Section 3 presents the results, Section 4 is the discussion, and Section 5 is the conclusion.

¹ https://www3.mpifr-bonn.mpg.de/staff/pfreire/NS_masses.html

2 DATA AND DATA REDUCTION

2.1 Data

There are 12 DNSs and one DNS candidate in the FAST sky. The information of these 13 sources are listed in Table 1. The observations were done with the FAST 19-beam receiver, which covers a frequency range of 1.05 to 1.45 GHz. The sampling time is 49.152 μ s, and the system temperature is \sim 24 K (Jiang et al. 2019). The data was channelized into 4096 channels and corresponding to 0.122 MHz channel width, which packetized and stored in search-mode PSRFITS format. We collected as many data as we can from FAST data archive (see details in the FAST observation catalog ²). The data spanning, the number of observations and total observing time of each source can be found in Table 2. The orbital phase coverage rate of each system is shown in Fig. 1. No eclipsing events are observed in any of our data.

Table 1: Information of the 13 DNS systems in the FAST sky.

Name	DM (pc cm ⁻³)	P (s)	P_b (days)	τ_{age} (Myr)	e	M_{TOT} (M_{\odot})	M_c (M_{\odot})	i ($^{\circ}$)
J0453+1559 ¹	30.30	0.04578	4.072	\sim 4100	0.11251847(8)	2.734(4)	1.174(4)	75.7 ^{+0.7} _{-0.8}
J0509+3801 ²	69.08	0.07654	0.380	\sim 200	0.586409(3)	2.81071(14)	1.412(6)	*
J1411+2551 ³	12.37	0.06245	2.616	\gtrsim 9100	0.1699308(4)	2.538(22)	> 0.92	*
J1518+4904 ⁴	11.61	0.04093	8.634	\gtrsim 16000	0.249484383(9)	2.7186(7)	1.248(⁺³⁵ ₋₂₉)	49.6 ^{+1.6} _{-1.8}
B1534+12 ⁵	11.62	0.03790	0.421	\sim 200	0.27367740(4)	2.678463(4)	1.3455(2)	77.7 \pm 0.9
J1759+5036 ²	7.78	0.17602	2.043	\sim 50000	0.30827(12)	2.679(12)	> 0.83	*
J1829+2456 ⁶	13.70	0.04101	1.176	\sim 12400	0.1391435(3)	2.60551(38)	1.299(7)	75.8 \pm 0.7
J1906+0746 ⁷	217.75	0.14407	0.166	\sim 0.112	0.0852996(6)	2.6134(3)	1.322(11)	43.7 \pm 0.5
J1913+1102 ⁸	338.96	0.02729	0.206	\sim 2800	0.089531(2)	2.8887(6)	1.27(3)	55.3
B1913+16 ⁹	168.77	0.05903	0.323	\sim 100	0.6171340(4)	2.828378(7)	1.390(1)	47.9 \pm 0.1
J1946+2052 ¹⁰	93.97	0.01696	0.078	\sim 290	0.0638180(6)	2.54(3)	> 1.2	*
B2127+11C ¹¹	67.13	0.03053	0.335	\sim 97	0.681395(2)	2.71279(13)	1.354(10)	65 \pm 2
J2150+3427 ¹²	55.48	0.65428	10.592	\sim 2880	0.601494(2)	2.59(13)	> 0.98	*

Note: The column, from left to right, list the DNS system name, dispersion measure, spin period, orbital period, characteristic age orbit eccentricity, the system mass, companion mass, and orbital inclination angle for each system. References: 1 (Martinez et al. 2015), 2 (McEwen et al. 2024), 3 (Martinez et al. 2017), 4 (Tan et al. 2024), 5 (Fonseca et al. 2014), 6 (Haniewicz et al. 2021), 7 (van Leeuwen et al. 2015), 8 (Ferdman et al. 2020), 9 (Weisberg & Huang 2016), 10 (Stovall et al. 2018), 11 (Jacoby et al. 2006; Wu et al. 2024), 12 (Wu et al. 2023).

2.2 Data Reduction

The PRESTO ³ (Ransom 2001; Ransom et al. 2002, 2003) was used to pre-process the data. The routine `rfifind` was used to mask radio frequency interference. The length of the data used to identify frequency domain interferences (-time option) was set to be 2 s. The `prepsubband` command was used to dedisperse the data around the pulsar's dispersion measure (DM). We generated eleven dedispersed time series for each observation, using DM values spaced by 0.1 pc cm⁻³ around the known pulsar's DM to ensure optimal

² <https://fast.bao.ac.cn/>

³ <https://github.com/scottransom/presto>

Table 2: Observation summaries of DNS systems

Name	Observation _{start} yyyy-mm-dd	Observation _{end} yyyy-mm-dd	Times	Total time hr
J0453+1559	2019-10-16	2021-10-23	11	30.0
J0509+3801	2020-05-04	2023-05-21	16	13.0
J1411+2551	2020-08-26	2023-04-11	8	4.1
J1518+4904	2019-10-22	2023-01-01	32	46.5
B1534+12	2020-08-26	2023-05-21	21	10.1
J1759+5036	2024-12-21	2024-12-21	1	1.8
J1829+2456	2019-10-17	2023-07-25	8	3.3
J1906+0746	2019-10-18	2023-04-15	23	39.5
J1913+1102	2020-09-11	2023-04-21	23	18.5
B1913+16	2019-10-19	2023-04-20	26	20.3
J1946+2052	2020-10-27	2024-11-01	26	36.1
B2127+11C	2019-11-09	2023-05-21	20	40.6
J2150+3427	2022-05-03	2023-04-24	30	8.4

Note: Columns 2 and 3 list the start and end dates of observations, respectively. Column 4 is for the total number of observations. Column 5 is for the cumulative observing time.

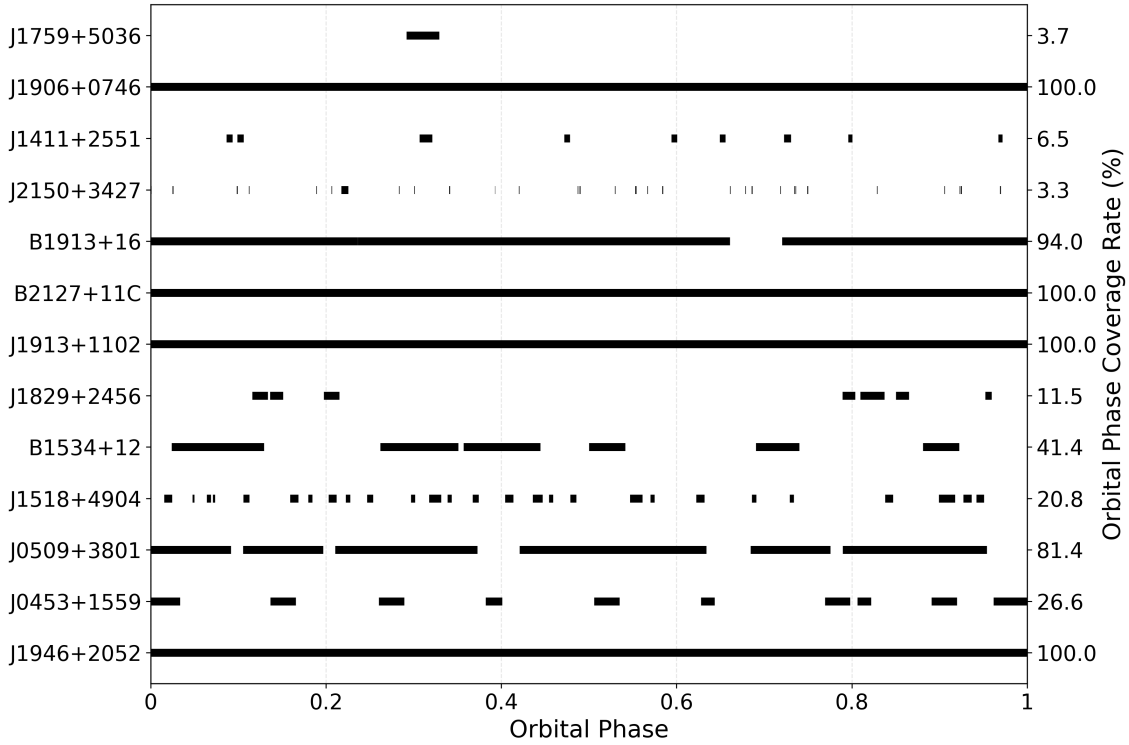


Fig. 1: The orbital phase coverage.

coverage for potential candidate detections. To avoid the influence of the pulsar's signal and its harmonics on the candidate identification in the search results, a birdie file was created to mask the pulsar's signal. The birdie masking is applied conservatively. The known pulsars are usually recycled pulsars (except for PSRJ1906+0746), while their companions are normal pulsars with longer periods than the known pulsars. We only mask the known pulsars and their low-order harmonics, if the companion signal could lie close

to or coincide with a harmonic of the known pulsar’s signal, which do not mask the companion’s signal completely.

The PYSOLATOR ⁴ (Ridolfi 2020) was used to correct the pulsar’s spin period variations induced by the orbital motion. It removes the orbital modulation by subtracting the predicted Roemer delay and resampling the time series, and resampling the data to the binary barycenter. It need the ephemeris file in which the total mass of the system (MTOT), companion mass (M2), and the sin value of the orbital inclination angle (SINI) should be included. In a double neutron star system, the projected semi-major axis of the companion pulsar, A_2 , generally differs from that of the known pulsar, A_1 . The two are related through the mass ratio $q = M_1/M_2 = A_2/A_1$ (M_1 and M_2 denote the masses of the known pulsar and its companion, respectively.), such that $A_2 = qA_1$. For 5 DNS systems among all the 13 in the FAST sky, the precise masses of the companion star and the orbital inclination angles have not been measured (see Table 1). Therefore, the canonical pulsar mass of $1.35 M_\odot$ in DNS systems (Kiziltan et al. 2013) was used as the companion mass, and the corresponding orbital inclination angle for such systems was adopted.

The RIPTIDE ⁵ (Morello et al. 2020) package was used to perform FFA pulsar searches via its `rffa` routine. The range of folding periods was set to be 0.001 – 60 seconds. The candidates with the $\text{SNR} \geq 7$ were selected for further analysis. The command `prepfold` from PRESTO was used to fold candidates.

Due to the relativistic spin precession, the interpulse of PSR J1946+2052 changed from a single-peak to a double-peak shape from 2018 to 2021 (Meng et al. 2024). Therefore, the timing solutions before 2018 are not applicable to the current observational data to remove orbital modulation. We performed a timing analysis for J1946+2052 with FAST observations. The `prepfold` routine was used to fold the data with parameters from the `parfile` of J1946+2052 (Stovall et al. 2018). The standard profile was from the Gaussian component fitting of the pulse profile from one of the 26 observational data of this pulsar with `pygaussfit.py`. The Time-of-arrivals (TOAs) were obtained using `get_TOA.py` routine from PRESTO. For the timing analysis, the APTB based on PINT (Susobhanan et al. 2024) software package is used to obtain a phase-connected timing solution.

3 RESULTS

3.1 The Timing Solution for J1946+2052

We used the 26 observational data from FAST. The time span is 1100 days, from 59149 to 60249. Our timing results and the previous one (Stovall et al. 2018) are presented in Table 3, while the timing residuals are showed in Fig. 2. Using these orbital parameters, we obtain the mass function of (e.g. Özel & Freire 2016)

$$f(m_p, m_c) = \frac{(m_c \sin i)^3}{(m_p + m_c)^2} = \frac{4\pi^2 x^3}{P_b^2 T_\odot} = 0.268137(2)M_\odot, \quad (1)$$

where $T_\odot = GM_\odot c^{-3} = 4.925490947 \mu\text{s}$, i is the inclination angle of the orbit, and m_p and m_c are the masses of the pulsar and its companion, respectively. For pulsars in compact binary systems, the measurement of PK parameters can further constrain the masses of the pulsar and the companion. We measured periastron advance $\dot{\omega}$ only, which is $25.8696(1) \text{ deg yr}^{-1}$. Assuming the periastron advance is caused by

⁴ https://alex88ridolfi.altervista.org/page/pulsar_software_PYSOLATOR.html

⁵ <https://github.com/v-morello/riptide>

the general relativistic effect alone, the rate of periastron advance should be (e.g. Stairs 2003)

$$\dot{\omega} = 3T_{\odot}^{2/3} \left(\frac{P_b}{2\pi} \right)^{-5/3} \frac{(m_p + m_c)^{2/3}}{1 - e^2}. \quad (2)$$

Thus, the total mass ($m_p + m_c$) was calculated as $2.54(3) M_{\odot}$, consistent with previous result (Stovall et al. 2018) and the newly high-precision timing result (Meng et al. 2025a).

Table 3: Comparison of timing parameters for PSR J1946+2052 between K. Stovall et al. (2018) and this work solution

	Stovall et al. (2018)	This Work
Right Ascension, α (J2000)	19:46:14.130(6)	19:46:14.13503(9)
Declination, δ (J2000)	+20:52:24.64(9)	+20:52:24.8999(3)
Spin Frequency, f (s^{-1})	58.9616546384(5)	58.961654623404(8)
1st Frequency Derivative, \dot{f} (s^{-2})	$-3.2(6) \times 10^{-15}$	$-3.7055(1) \times 10^{-15}$
2nd Frequency Derivative, \ddot{f} (s^{-3})	–	$-1.2(8) \times 10^{-24}$
Reference Epoch (MJD)	57989.0	57989.0
Dispersion Measure, DM ($pc\ cm^{-3}$)	93.965(3)	93.965
Solar System Ephemeris	DE436	DE421
Terrestrial Time Standard	TT(BIPM)	TT(BIPM2023)
Time Units	TDB	TDB
Span of Timing Data (MJD)	57953–58024	59149–60249
Residuals RMS (μs)	95.04	42.53
Number of TOAs	–	364
Binary Parameters		
Binary Model	DD	DD
Orbital Period, P_b (days)	0.07848804(1)	0.0784880558834(4)
Projected Semi-major Axis, x_p (lt-s)	1.154319(5)	1.1544228(4)
Eccentricity, e	0.063848(9)	0.0638180(6)
Longitude of Periastron, ω (deg)	132.88(1)	132.527(4)
Epoch of Periastron, T_0 (MJD)	57989.002943(3)	57989.0028971(9)
Periastron Advance, $\dot{\omega}$ ($deg\ yr^{-1}$)	25.6(3)	25.8696(1)
Mass Function, f_{mass} (M_{\odot})	0.268184(12)	0.268137(2)
Total System Mass, M_{Total} (M_{\odot})	2.50(4)	2.54(3)

3.2 The Search Results

We successfully removed the orbital effects of all the 13 DNS systems in FAST sky using PYSOLATOR. Fig. 3 shows the signals of the 12 pulsars in the DNS systems, after the orbital effects were removed. For J1946+2052, the pulsar period in every observation still varies slightly due to the errors from the timing solution. As the period variation introduces phase drift, it leads to pulse broadening and has an unknown impact on the sensitivity of the FFA-based search. Some folding results from its resampled data can be found in Fig.2 as examples. We also aim to achieve more precise timing solutions (such as the result of Meng et al. 2025b), and the orbital effects can be further minimized or fully removed in future analyses.

We searched for the companion periodic radio signals of the 13 DNS systems, with a total of 245 observational data and a duration of 272.2 hours (see Table 2). As a result, 197962 candidates were found from all the data. Every candidate was checked carefully and none was confirmed as the companion signals.

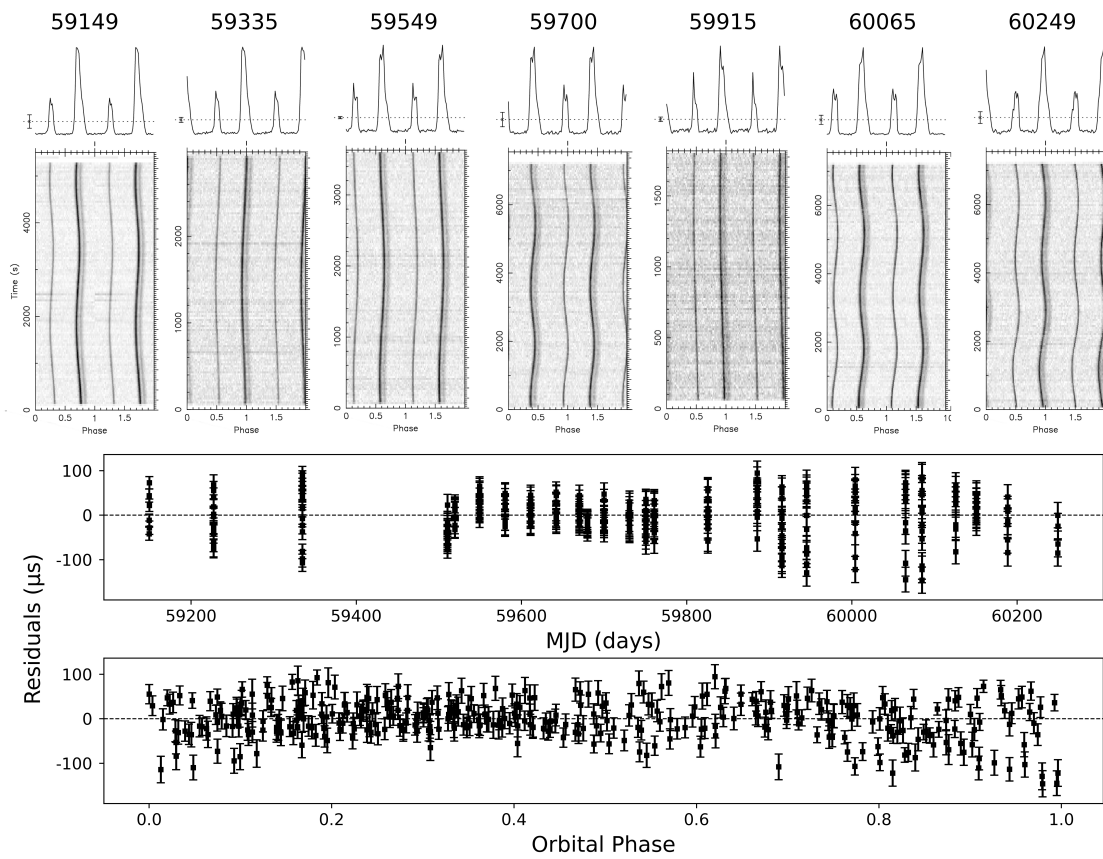


Fig. 2: The pulse profile (upper subplot) and the timing residual as a function of MJD and orbital phase from the best-fit timing model (lower subplot) with PSR J1946+2052.

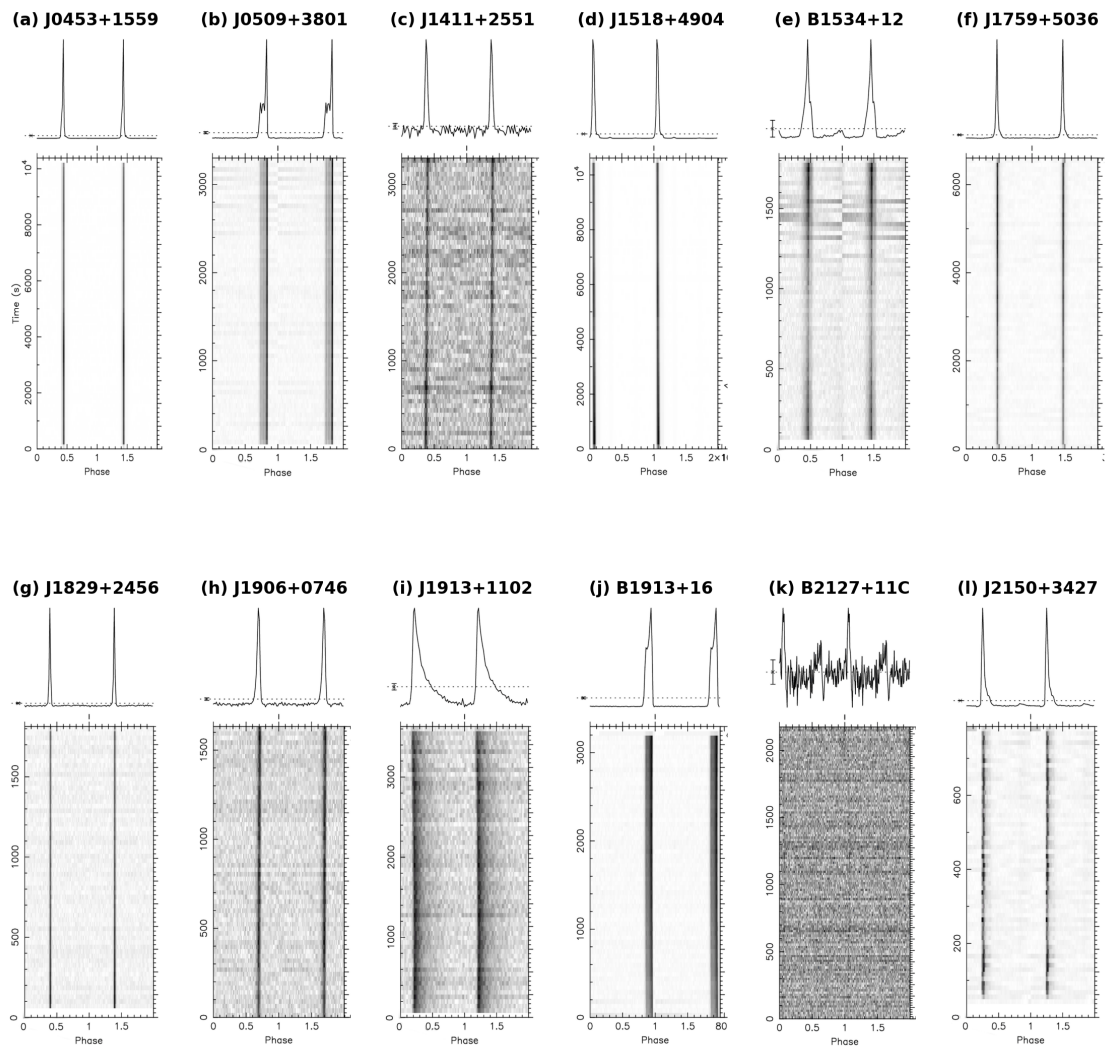


Fig. 3: The pulse profiles of the primary stars in 12 DNS systems, the results of FFA search after the orbital effects were removed.

4 DISCUSSION

4.1 The Search Sensitivities

The search sensitivities were estimated using the radiometer equation (e.g. Dewey et al. 1985)

$$S_{\min} = \beta \frac{(S/N_{\min}) T_{\text{sys}}}{G \sqrt{n_p T_{\text{obs}} \Delta f}} \sqrt{\frac{W_{\text{obs}}}{P - W_{\text{obs}}}}, \quad (3)$$

in which the β is the sampling efficiency (here we use 1 for the 8-bit recording system), the (S/N_{\min}) is the minimum signal-to-noise ratio (being 7 in our search), the number of polarizations (n_p) is 2, the T_{obs} is the integration time in seconds, the W_{obs} is the width of the pulsar profile, the P is the spin period of pulsar. For FAST, the system temperature (T_{sys}) is 24 K, the antenna gain, G , is 16 K Jy^{-1} , the Δf is the bandwidth in the unit of MHz, here is 400 MHz (Jiang et al. 2019). The parameters of some other radio telescopes are listed in Table 4. Assuming the W_{obs} is 3% for long period pulsars, the sensitivity varying with different DM values and spin periods was present in Fig. 4. As the orbital effects removed, the observing time (here we used is 2 hour) was used instead of considering the orbital effects during pulsar search.

FAST no doubt exhibits the highest sensitivity among all the telescopes. When the DM value is 350 pc cm^{-3} , the sensitivity decreased a lot when the spin period is 2 ms or shorter. Thus, excluding the situation that the companion is a very fast millisecond pulsar, our search reached a higher sensitivity.

On the other hand, the single pulse search will break such sensitivity estimation, while the aperture is the most important parameter. Geodetic precession of the orbit may enhance detectability, which should be taken into account in the future.

Table 4: Telescope parameters used in sensitivity calculations

Telescope	β	T_{sys} (K)	G (K Jy^{-1})	Δf (MHz)	ν_{center} (GHz)	Channels	Frequency range (GHz)
FAST ¹	1.0	24.0	16.0	400	1.25	4096	1.05–1.45
Arecibo ²	1.2	40.0	10.5	300	1.40	256 (512)	1.15–1.55
MeerKAT ³	1.1	26.0	2.8	650	1.284	1024	0.96–1.60
GBT ⁴	1.05	22.8	2.0	650	1.50	512	1.18–1.83
uGMRT ⁵	1.0	102.5	4.2	180	0.65	4096	0.56–0.74
Parkes ⁶	1.5	35.0	0.7	288	1.374	96	1.23–1.52

Note: Column 2 lists the sampling efficiency that accounts for various sensitivity losses due to signal processing and digitization. Columns 3 and 4 list the system temperature and antenna gain, and Columns 5 and 6 list the bandwidth and central observing frequency. Column 7 lists the number of channels, Column 8 lists the low- and high-frequency edges of the bandwidth. To optimize channel selection, we set channels to be 256 if the DM value is $< 100 \text{ pc cm}^{-3}$. For higher DM values ($> 100 \text{ pc cm}^{-3}$), we set channels to be 512, ensuring sufficient resolution. References: 1 (Jiang et al. 2019), 2 (Hessels et al. 2007), 3 (Ridolfi et al. 2021), 4 (Martsen et al. 2022), 5 (Gautam et al. 2022), 6 (Camilo et al. 2000).

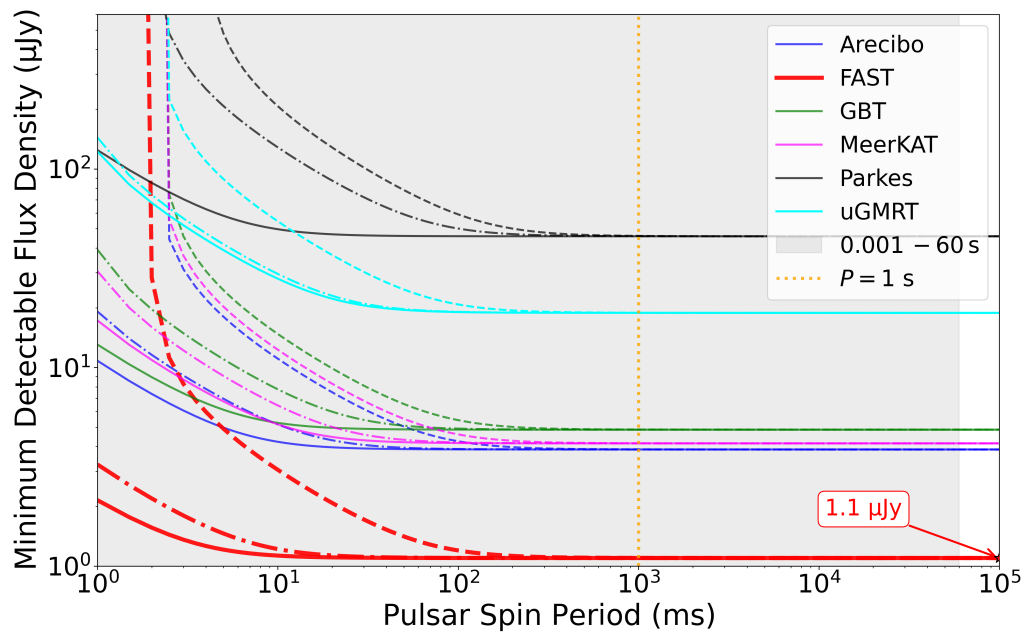


Fig. 4: Survey sensitivity as a function of pulsar period and DM when the observation time is 2 hours for all the telescopes, assuming an intrinsic pulse width of 3 %. The solid line, dash-dot line, and dash line in every colour represent the DM values of 10, 200, and 350 pc cm^{-3} , respectively, as these three numbers are the lowest, median, and highest DM values among all the selected 13 pulsars in our study. The shaded area represents the searched pulsar period range.

4.2 FFA Plus PYSOLATOR

The FFA shows significant advantages in searching for long-period pulsars with long spin periods ($P \sim 1$ s) compared to the traditional FFT-based method (Cameron et al. 2017). This advantage arises from its time-domain folding technique, which avoids the sensitivity loss caused by red noise in FFT-based searches. Furthermore, FFA produces fully phase-coherent folded pulse profiles, while FFT methods can only incoherently sum a limited number of harmonics (typically 16–32), leaving part of power unused. In terms of computational efficiency, FFA scales as $O(N \log_2(N/P_0))$ (Cameron et al. 2017), where N is the number of data samples and P_0 is the base trial period. As P_0 increases, FFA becomes increasingly efficient, making it well-suited for systematic searches of isolated, long-period pulsars.

Despite these advantages, FFA has difficulties in searching compact binary systems such as DNS systems. The orbital motion of the pulsar induces Doppler shifts that cause changes in the rotation period of pulsar. Thus, the sensitivity of FFA searches is reduced. In the frequency domain, the acceleration search techniques (Andersen & Ransom 2018; Cameron 2018) partially mitigate this problem by approximating the orbital acceleration as constant over a small fraction of the orbital period. However, their performance deteriorates significantly when large values of the z_{\max} (maximum Fourier drift parameter) are required, limiting their efficiency for highly accelerated systems.

To address this challenge, the code PYSOLATOR can be used to resample the time-series data with the orbital parameters of the DNS system and thus removes the pulsar spin period variation. This approach restores the phase coherence of the signal and maximizes both the sensitivity and computational efficiency of the search, even in strongly accelerated binary systems. The S/N values in table 5 show that after resampling the S/N were at least 30% higher than before. Among these signals, the periodic signal of B2127+11C can only be detected using the FFA after removing the orbital modulation effects. These results indicate that the combined use of PYSOLATOR and FFA can enhance the search sensitivity of companion stars in DNS systems. Applying our pipeline to all publicly available pre-2008 archival observations of double pulsar J0737–3039A/B successfully recovers the periodic signal of pulsar A, while no detectable signal from pulsar B is present in the observational data; this is consistent with the well-known intermittency and long-term disappearance of pulsar B due to relativistic spin precession, indicating that the nondetection reported here reflects existing observational constraints rather than a limitation of the pipeline.

4.3 The Narrow Radiation Beam of Companion Star

In DNS systems, the second-formed neutron star (companion star) is usually a non-recycled (Tauris et al. 2017), often possessing a long spin period and narrow beam opening angle. The beam opening angle is increase as the spin period P decreases, and can be approximately estimated as

$$\rho \approx 5.4^\circ P^{-0.5} \quad (4)$$

(Tauris & Manchester 1998; Rankin 1990). So, a millisecond pulsar with a spin period of 0.01 s may have a beam opening angle of 54° , while a pulsar with a 1 s period would have an opening angle of only about 5.4° . This supports the observational phenomenon that most detected pulsar in DNS systems are recycled pulsars, while the companion star is often unseen. In addition, for pulsars with narrow pulses (duty cycle $\delta < 1\%$),

Table 5: Basic Information and SNR Changes of Double Neutron Star Systems

Name	Obs Date	Spin	Obs	S/N	S/N
	yyyy-mm-dd	Period (s)	Duration (s)	Before	After
J0453+1559	2021-10-21	0.04578	10200	2442.9	5525.4
J0509+3801	2022-05-05	0.07654	5400	195.9	775.3
J1411+2551	2023-04-11	0.06245	3300	28.4	59.3
J1518+4904	2021-11-18	0.04093	10500	7018.8	9422.2
B1534+12	2023-05-21	0.03790	1800	68.2	214.2
J1759+5036	2024-12-21	0.17602	6600	687.8	973.8
J1829+2456	2023-07-25	0.04101	1800	82.8	214.2
J1906+0746	2020-09-02	0.14407	1800	26.6	140.0
J1913+1102	2022-01-20	0.02729	3600	45.9	155.4
B1913+16	2023-01-05	0.05903	3200	227.0	1589.7
J1946+2052	2024-11-01	0.01696	6600	38.7	241.5
B2127+11C	2019-11-09	0.03053	4800	*	7.2
J2150+3427	2022-10-31	0.65427	7335	130.1	171.7

Note: Column 2 lists the observation date of each double neutron star (DNS) source; Column 3 lists the spin period of the primary star; Column 4 lists the observation duration; Columns 5 and 6 list the signal-to-noise ratios (S/N) obtained by FFA before and after resampling with PYSOLATOR, respectively. * denotes no valid data.

more energy in the frequency domain is distributed in harmonics. Searching in frequency domain will lose more energy (Cameron et al. 2017) due to the limited number of harmonic superpositions. Therefore, FFA is no doubt suitable for searching such periodic signals of companion stars.

It is worth noting that the detected pulsar in J1906+0746 is a young one, indicating that its companion can be a recycled pulsar with relatively short spin period and wide beam opening angle, will be visible as a double pulsar in the future (Wang & van Leeuwen 2025). In addition, as in the extremely dense core-collapsing globular cluster M15, the companion of B2127+11C may also be a recycled one. Thus, in FAST sky, these two targets should have higher priority in the companion signal search.

4.4 Geodetic Precession

Geodetic precession, predicted by general relativity, causes a pulsar’s spin axis (and radio beam) to gradually change direction. The geodesic precession rates of five DNS systems are listed in Table 6. This phenomenon influences whether the companion’s radio emission can be detected in DNS systems. For example, PSR J0737–3039B has not been visible after 2008 (Perera et al. 2012), B1913+16 is expected to disappear around 2025 (Kramer 2003), and B2127+11C may become visible again between the year 2041 and 2053 (Ridolfi et al. 2018). Therefore long-term timing observations combined with precession geometry modeling can be used to predict visibility windows and identify epochs when periodic signals become detectable.

Similar to the previous subsection, pulsar J1906+0746 and B2127+11C with more than $1^\circ/\text{yr}$ geodetic precessions. With the $\sim 8^\circ/\text{yr}$, it is also important to perform long term observation of J1946+2052.

Table 6: DNS systems with geodetic precession

Name	Geodetic Precession ($^{\circ}/\text{yr}$)
B1534+12 ¹	0.59($^{+0.12}_{-0.08}$)
J1906+0746 ²	2.17 \pm 0.11
B1913+16 ³	1.21
J1946+2052 ⁴	7.96
B2127+11C ⁵	1.31

Note: This table lists DNS systems for which geodetic precession values have been measured. References: 1 (Fonseca et al. 2014), 2 (Desvignes et al. 2019), 3 (Kramer 1998), 4 (Meng et al. 2024), 5 (Kirsten et al. 2014).

4.5 Other newly discovered DNS Systems

There are four newly DNS systems (or DNS candidates): J1953+1847D (Lian et al. 2025) in globular cluster M71, J1901+0658 (Su et al. 2024), J0528+3529 and J1844-0128 (Wang et al. 2025) were discovered by FAST (the basic parameter see Table 7). The FAST globular cluster pulsar survey have enough M71 data and we will search for the companion signal soon. For other three, no available archive data found.

Table 7: Basic parameters of four recently reported DNS systems.

Name	DM (pc cm^{-3})	Spin Period (s)	P_b (days)	τ_{age} (Myr)	e	M_{TOT} (M_{\odot})	M_c (M_{\odot})
J1953+1847D (M71D) ¹	117.7	0.10068	10.938	> 8800	0.628921(3)	2.63(8)	> 1.29
J1901+0658 ²	125.9	0.07574	14.455	\sim 5500	0.3662392(5)	2.79(7)	> 1.11
J0528+3529 ³	111.8	0.07823	11.726	\sim 1686	0.2901088(10)	2.90(12)	> 1.15
J1844-0128 ³	138.3	0.02914	4.188	\sim 1500	0.234949(5)	1.7(8)	> 0.72

Note: Parameters are taken from the timing analyses in the cited papers. The columns represent, respectively, dispersion measure, spin period, orbital period, characteristic age, orbital eccentricity, total system mass, and companion mass. References: 1 (Lian et al. 2025), 2 (Su et al. 2024), 3 (Wang et al. 2025).

5 CONCLUSION

The conclusions of our study are as follows:

1. We introduced a FFA-based binary pulsar search pipeline, aiming to find the periodic signals of the companion stars in the DNS systems. As most of these systems have a detected recycled pulsar and a highly possible normal (long spin period) pulsar, we suggest that FFA-based pulsar search should obtain higher sensitivity.

2. We searched most of the archived FAST data of the 13 DNS systems, with no candidate found.

3. The timing of pulsar J1946+2052 may not be precise enough for orbital movement removal, thus we infer that maybe the FFT based or even spectra stacking (e.g. Pan et al. 2016) may have chance to find its companion signal.

4. The geodetic precession may result in the next double pulsar. The candidate can be J1906+0746 (2.17 $^{\circ}/\text{yr}$) and J1946+2052 (7.96 $^{\circ}/\text{yr}$).

5. In the future, we plan to search for the single pulses of DNS systems and determine whether the single pulses come from the companion star by comparing the pulse phase of the single pulses with that of the known pulsar.

Acknowledgements We thank the referee’s valuable suggestions, which helped to refine our paper. We are grateful to Alessandro Ridolfi for his helpful suggestions and assistance in clarifying several technical aspects of PYSOLATOR. This work is supported by the National Key R & D Program of China No. 2022YFC2205202, No. 2020SKA0120100, and the National Natural Science Foundation of China (NSFC, Grant Nos. 12373032, 12003047, 11773041, U2031119, 12173052, and 12173053. Both Lei Qian and Zhichen Pan were supported by the Youth Innovation Promotion Association of CAS (id. 2018075, Y2022027, and 2023064) and the CAS “Light of West China” Program. Liyun Zhang has been supported by the Science and Technology Program of Guizhou Province under project No.QKHPTRC-ZDSYS[2023]003 and QKHFQ[2023]003. This work made use of the data from FAST (Five-hundred-meter Aperture Spherical radio Telescope) (<https://cstr.cn/31116.02.FAST>). FAST is a Chinese national mega-science facility, operated by the National Astronomical Observatories, Chinese Academy of Sciences. We sincerely appreciate all the PIs of the FAST archival data used in this work.

References

- Abbott, B. P., Abbott, R., Abbott, T. D., et al. 2017, *Phys. Rev. Lett.*, 119, 161101 2
- Andersen, B. C., & Ransom, S. M. 2018, *ApJ*, 863, L13 11
- Breton, R. P., Kaspi, V. M., Kramer, M., et al. 2008, *Science*, 321, 104 2
- Burgay, M., D’Amico, N., Possenti, A., et al. 2003, *Nature*, 426, 531 2
- Cameron, A. D. 2018, Innovative pulsar searching techniques : or fantastic pulsars and how to find them, Ph.D. thesis, Rheinische Friedrich Wilhelms University of Bonn, Germany 11
- Cameron, A. D., Barr, E. D., Champion, D. J., Kramer, M., & Zhu, W. W. 2017, *MNRAS*, 468, 1994 11, 12
- Camilo, F., Lorimer, D. R., Freire, P., Lyne, A. G., & Manchester, R. N. 2000, *ApJ*, 535, 975 9
- Desvignes, G., Kramer, M., Lee, K., et al. 2019, *Science*, 365, 1013 13
- Dewey, R. J., Taylor, J. H., Weisberg, J. M., & Stokes, G. H. 1985, *ApJ*, 294, L25 9
- Ferdman, R. D., Freire, P. C. C., Perera, B. B. P., et al. 2020, *Nature*, 583, 211 3
- Fonseca, E., Stairs, I. H., & Thorsett, S. E. 2014, *ApJ*, 787, 82 3, 13
- Gautam, T., Ridolfi, A., Freire, P. C. C., et al. 2022, *A&A*, 664, A54 9
- Haniewicz, H. T., Ferdman, R. D., Freire, P. C. C., et al. 2021, *MNRAS*, 500, 4620 3
- Hessels, J. W. T., Ransom, S. M., Stairs, I. H., Kaspi, V. M., & Freire, P. C. C. 2007, *ApJ*, 670, 363 9
- Hulse, R. A., & Taylor, J. H. 1975, *ApJ*, 195, L51 1
- Jacoby, B. A., Cameron, P. B., Jenet, F. A., et al. 2006, *ApJ*, 644, L113 3
- Jiang, P., Yue, Y., Gan, H., et al. 2019, *Science China Physics, Mechanics, and Astronomy*, 62, 959502 3, 9
- Keane, E., Bhattacharyya, B., Kramer, M., et al. 2015, in *Advancing Astrophysics with the Square Kilometre Array (AASKA14)*, 40 2
- Kirsten, F., Vlemmings, W., Freire, P., et al. 2014, *A&A*, 565, A43 13

- Kiziltan, B., Kottas, A., De Yoreo, M., & Thorsett, S. E. 2013, *ApJ*, 778, 66 5
- Kramer, M. 1998, *ApJ*, 509, 856 13
- Kramer, M. 2003, in *Nonlinear Gravitodynamics: The Lense-Thirring Effect*. Edited by RUFFINI REMO & SIGISMONDI COSTANTINO. Published by World Scientific Publishing Co. Pte. Ltd, edited by R. Ruffini & C. Sigismondi, 505–509 12
- Kramer, M., & Stairs, I. H. 2008, *ARA&A*, 46, 541 2
- Kramer, M., Stairs, I. H., Manchester, R. N., et al. 2021, *Physical Review X*, 11, 041050 2
- Lattimer, J. M., & Prakash, M. 2016, *Phys. Rep.*, 621, 127 2
- Li, Y., Wang, L., Qian, L., et al. 2025, *ApJ*, 991, 38 2
- Lian, Y., Pan, Z., Zhang, H., et al. 2025, *ApJS*, 279, 51 2, 13
- Lyne, A. 2004, in *AAS/High Energy Astrophysics Division #8, AAS/High Energy Astrophysics Division*, vol. 8, 11.01 2
- Martinez, J. G., Stovall, K., Freire, P. C. C., et al. 2015, *ApJ*, 812, 143 3
- Martinez, J. G., Stovall, K., Freire, P. C. C., et al. 2017, *ApJ*, 851, L29 3
- Martsen, A. R., Ransom, S. M., DeCesar, M. E., et al. 2022, *ApJ*, 941, 22 9
- McEwen, A. E., Swiggum, J. K., Kaplan, D. L., et al. 2024, *ApJ*, 962, 167 3
- Meng, L., Freire, P. C. C., Stovall, K., et al. 2025a, arXiv e-prints, arXiv:2510.12506 6
- Meng, L., Freire, P. C. C., Stovall, K., et al. 2025b, *A&A*, 704, A153 6
- Meng, L., Zhu, W., Kramer, M., et al. 2024, *ApJ*, 966, 46 5, 13
- Morello, V., Barr, E. D., Stappers, B. W., Keane, E. F., & Lyne, A. G. 2020, *MNRAS*, 497, 4654 2, 5
- Nan, R., Li, D., Jin, C., et al. 2011, *International Journal of Modern Physics D*, 20, 989 2
- Özel, F., & Freire, P. 2016, *ARA&A*, 54, 401 5
- Pan, Z., Hobbs, G., Li, D., et al. 2016, *MNRAS*, 459, L26 13
- Perera, B. B. P., Lomiashvili, D., Gourgouliatos, K. N., McLaughlin, M. A., & Lyutikov, M. 2012, *ApJ*, 750, 130 12
- Rankin, J. M. 1990, *The Emission Geometry, Radiation Processes, and Evolution of Radio Pulsars*, NSF Award Number 8917722. Directorate for Mathematical and Physical Sciences, Division Of Astronomical Sciences. 1990. 11
- Ransom, S. M. 2001, *New search techniques for binary pulsars*, Ph.D. thesis, Harvard University, Massachusetts 3
- Ransom, S. M., Cordes, J. M., & Eikenberry, S. S. 2003, *ApJ*, 589, 911 3
- Ransom, S. M., Eikenberry, S. S., & Middleditch, J. 2002, *AJ*, 124, 1788 3
- Ridolfi, A. 2020, *PYSOLATOR: Remove orbital modulation from a binary pulsar and/or its companion*, Astrophysics Source Code Library, record ascl:2003.012 5
- Ridolfi, A., Freire, P. C. C., Kramer, M., et al. 2018, in *Pulsar Astrophysics the Next Fifty Years, IAU Symposium*, vol. 337, edited by P. Weltevrede, B. B. P. Perera, L. L. Preston, & S. Sanidas, 251–254 12
- Ridolfi, A., Gautam, T., Freire, P. C. C., et al. 2021, *MNRAS*, 504, 1407 9
- Staelin, D. H. 1969, *IEEE Proceedings*, 57, 724 2
- Stairs, I. H. 2003, *Living Reviews in Relativity*, 6, 5 6

- Stovall, K., Freire, P. C. C., Chatterjee, S., et al. 2018, *ApJ*, 854, L22 3, 5, 6
- Su, W. Q., Han, J. L., Yang, Z. L., et al. 2024, *MNRAS*, 530, 1506 2, 13
- Susobhanan, A., Kaplan, D. L., Archibald, A. M., et al. 2024, *ApJ*, 971, 150 5
- Tan, C. M., Fonseca, E., Crowter, K., et al. 2024, *ApJ*, 966, 26 3
- Tauris, T. M., Kramer, M., Freire, P. C. C., et al. 2017, *ApJ*, 846, 170 2, 11
- Tauris, T. M., & Manchester, R. N. 1998, *MNRAS*, 298, 625 11
- Tauris, T. M., & van den Heuvel, E. P. J. 2006, in *Compact stellar X-ray sources*, vol. 39, edited by W. H. G. Lewin & M. van der Klis, 623–665 (Cambridge University Press) 2
- Taylor, J. H., & Weisberg, J. M. 1982, *ApJ*, 253, 908 2
- van Leeuwen, J., Kasian, L., Stairs, I. H., et al. 2015, *ApJ*, 798, 118 3
- Wang, P. F., Han, J. L., Yang, Z. L., et al. 2025, *Research in Astronomy and Astrophysics*, 25, 014003 2, 13
- Wang, Y., & van Leeuwen, J. 2025, *A&A*, 701, A180 12
- Weisberg, J. M., & Huang, Y. 2016, *ApJ*, 829, 55 3
- Wu, Q. D., Wang, N., Yuan, J. P., et al. 2023, *ApJ*, 958, L17 2, 3
- Wu, Y., Pan, Z., Qian, L., et al. 2024, *ApJ*, 974, L23 2, 3